Multimed Tools Appl (2015) 74:8961–8977
DOI 10.1007/s11042-013-1570-1

# Digital image super-resolution using adaptive interpolation based on Gaussian function

**Muhammad Sajjad · Naveed Ejaz · Irfan Mehmood · Sung Wook Baik**

Published online: 9 July 2013
© Springer Science+Business Media New York 2013

**Abstract** This paper presents a new approach to digital image super-resolution (SR). Image SR is currently a very active area of research because it is used in various applications. The proposed technique uses Gaussian edge directed interpolation to determine the precise weights of the neighboring pixels. The standard deviation of the interpolation window determines the value of the sigma 'σ' for generating Gaussian kernels. Therefore, the proposed scheme adaptively applies different Gaussian kernels according to the computed standard deviation of the interpolation window. Laplacian is applied to the image generated by the Gaussian kernels to enhance the visual quality of the output image. It has the significant benefit of being isotropic i.e. invariant to rotation. These features of being isotropic not only resemble human visual perception but also respond to intensity variations equally in all directions for any kind of kernel. It highlights the discontinuities of high frequencies in the image generated by the Gaussian kernel and deemphasizes the regions with slowly varying luminance levels. It also recovers the background missing features while preserving the sharpness of the output image. The proposed scheme preserves geometrical regularities across the boundaries and smoothes intensities inside the high frequencies. It also maintains the textures inside geometrical regularities. Therefore, high resolution (HR) images produced by the proposed scheme contain intensity information very close to the original details of the low-resolution (LR) image i.e. edges, smoothness and texture information. Various evaluation metrics have been applied to compute the validity of the proposed technique. Extensive experimental comparisons with state-of-the-art zooming schemes validate the claim of the proposed technique of being superior. It produces high quality at the cost of low time complexity.

M. Sajjad · N. Ejaz · I. Mehmood · S. W. Baik (✉)
College of Electronics and Information Engineering, Sejong University, Seoul, Korea
e-mail: sbaik@sejong.ac.kr

M. Sajjad
e-mail: sajjad@sju.ac.kr

N. Ejaz
e-mail: naveed@sju.ac.kr

I. Mehmood
e-mail: irfanmehmood@sju.ac.kr

**Keywords** Digital image magnification · Super-resolution · Laplacian · Gaussian kernel · Gaussian sigma · Weighted interpolation · Human visual perception

## 1 Introduction

Image SR means to take an LR image as an input and generate a corresponding HR image. The terms zooming, image reconstruction, digital image magnification (DIM) and upscaling etc. are used interchangeably for the same process. Image SR aims to compute HR images containing accurate and precise details of the original LR image. Image SR schemes must preserve the high frequency information, texture, geometrical regularities, and smoothness of the original input image while producing s HR image from the source input image. Image SR has various applications in many areas e.g. high-definition television (HDTV) [30], medical imaging [31], surveillance systems, satellite-imaging, and entertainment etc. A variety of techniques can be used to produce an SR image. The reconstruction based SR schemes [6, 15, 17, 22, 27] need prior information to model the zooming scheme. This information can be acquired by down-sampling the HR images to LR images. In order to construct the HR image from the input source image, the process of reconstruction is considered as the inverse problem by adding one or more LR images. In reconstruction-based schemes, the quality of the SR image is usually quite poor due to registration problems and map models used for prior knowledge. There are various image magnification techniques based on machine learning approaches [9, 17, 19, 22, 24, 33, 36]. For this purpose, a set of LR patches and their corresponding HR image patches are stored in the database. A patch of an HR image is recovered from its corresponding LR patch using features such as descriptor information stored in the database. Machine learning based approaches have certain limitations due to the dependency on various parameters e.g. dictionary size, size of atoms and type of images used for training. They are also highly complex and it is very difficult to incorporate them in real time applications. There must be a tradeoff between time complexity and image quality. Interpolation based image SR schemes [12, 21, 26, 32, 35] are used most often. Such techniques take a single image as an input and produce a HR image. The common interpolation techniques are the nearest neighbor (NN), bilinear and bicubic. These techniques are non-adaptive. The time complexity of these non-adaptive techniques is low but they introduce some unwanted artifacts across the edges in the output HR image. There are some edge-directed interpolation schemes [18, 20, 21, 26, 37], which are adaptive and preserve the original details of the source image. Moreover, these techniques perform the interpolation in selective directions using the geometrical and structural information of the image. A bicubic interpolation scheme is used most frequently due its low time complexity and good visual results. [18] proposed a zooming technique using a block-expanding method based on intervals which associate each pixel with an interval acquired by a weighted combination of the pixels in the vicinity. It overly sharpens the HR image and produces edge halo aliasing effects around the edges.

In this paper, our objective is to develop an efficient SR scheme that constructs an HR image of high visual quality from a given LR source image. The idea of the proposed technique is based on a computation of the unknown pixels from given known pixels in the neighborhood by weighted approximation. In order to assign the correct weight to each pixel in the neighborhood [8, 11, 18], the weights are generated by Gaussian kernel. It approximates the accurate value of the unknown pixels by giving the precise weight to each pixel in the near vicinity. For this purpose, the proposed technique uses two types of Gaussian kernels, generated by two different values of sigma of a Gaussian function. The standard

deviation of the interpolated window determines the type of Gaussian kernel to be used. The quality of the output image is further enhanced by deploying the properties of Laplacian. It has an equal effect in all directions on the intensity variation for any kind of kernel because of it being isotropic. It highlights the discontinuities of sharp luminance variations in the image produced by Gaussian kernels of the proposed technique and deemphasizes the regions with slowly varying intensity levels. It also recovers the missing features in the background of the output image while maintaining its geometrical regularities. Extensive quantitative and qualitative comparisons with state-of-the-art SR schemes validate the effectiveness of the proposed scheme. It is very simple computationally and resembles classic interpolation techniques, but has better quality than classic interpolation schemes. It can be easily incorporated in the applications that need real time response.

In section 2, the related work is described briefly. The proposed method is explained in detail in section 3. In section 4, the experimental results are discussed and the paper is concluded in section 5.

## 2 Related work

In this section, we describe some state-of-the-art image SR schemes. Various well known applications such as Adobe Photoshop, Windows Photo Viewer, etc. [4, 16] use many classic interpolation schemes. NN is one of the most simple non-adaptive interpolation schemes. It has the least amount of running time because it considers the nearest pixel in the vicinity of the interpolated pixel. It is also called "pixel replication" because it simply replicates the values of the known pixel in the HR image. It produces undesirable artifacts in the HR image, such as blocking effects, staircases, etc. A bit more complicated and better than NN is bilinear, because it incorporates the nearest 2×2 neighboring pixels of the interpolated pixel. In each dimension, it computes two linear interpolation functions. Assume that $S$ is a two dimensional image, for an arbitrary resampling pixel $(x, y)$ in $S$, the interpolation functions of bilinear are:

$$\begin{aligned} S_{y1} &= S_{11} + \frac{S_{21}-S_{11}}{x_2-x_1}(x-x_1) \\ S_{y2} &= S_{12} + \frac{S_{22}-S_{12}}{x_2-x_1}(x-x_1) \\ S(x,y) &= S_{y1} + \frac{S_{y2}-S_{y1}}{y_2-y_1}(y-x_1) \end{aligned} \tag{1}$$

The HR image magnified by bilinear interpolation is better than NN but it also suffers from aliasing effects. Bicubic scheme goes one step beyond the bilinear algorithm by considering 4×4 neighboring pixels in the vicinity of the interpolated pixel. It considers sixteen pixels in total for the interpolation process (http://www.cambridgeincolour.com/tutorials/image-interpolation.htm). The pixels near the interpolated pixel get the higher weights in the interpolation process. The interpolated point can be computed as

$$S(x,y) = \sum_{i=1}^{4}\sum_{j=1}^{4} w_{i,j} S\left(x_i, y_j\right) \tag{2}$$

In both x and y directions and also across the four corners of the interpolation window, the gradients are calculated. It produces 16 equations which compute the weights $w_{i,j}$ of the corresponding sixteen pixels. Bicubic interpolation produces more attractive results than

bilinear and NN. That is why it is the standard in many image editing programs such as Adobe Photoshop, printer drivers and in camera interpolation. However, it also suffers from distortion and blurring effects. Many edge-directed interpolation schemes have been proposed to cover the shortcomings of the classic interpolation techniques. Lee and Yoon [37] presented an edge-directed up-sampling method based on the radial basis function interpolation. It is an adaptive non-linear scheme and computes the interpolated point according to the information in the underlying edges. Jurio et al. [18] proposed a non-linear interpolation scheme that incorporates each pixel with an interval $f(Q_{i,j}, \delta.w)$ obtained by weighted aggregation of the pixels in its vicinity.

$$f\left(Q_{i,j}, \delta{\cdot}w\right) = \left[Q_{i,j}(1-\delta{\cdot}w), Q_{i,j}(1-\delta{\cdot}w) + \delta{\cdot}w\right] \tag{3}$$

$w$ is the intensity difference between the largest and smallest pixels in the interpolation window. The SR image can be obtained from the interval with a linear operator $K_\alpha$. The reader can find more detail about $K_\alpha$ and $f(Q_{i,j}, \delta.w)$ in [18]. It over sharpens the HR image by generating edge halo artifacts around the edges. Machine learning-based algorithms have been developed to minimize the aliasing effects of zooming schemes. Gajjar and Joshi [9] proposed a new discrete wavelet transformation-based approach that learns a set of basis functions from a group of LR images and their corresponding HR images. Yang et al. [36] proposed an image SR method using sparse coding concepts. It learns dictionaries for two feature spaces i.e. LR feature space and HR feature space. First it recovers sparse representation $\alpha$ for each LR patch $P_{LR}$ from the LR dictionary $D_{LR}$ and then computes the corresponding HR patch $P_{HR}$ as a sparse linear combination with respect to the HR dictionary $D_{HR}$ i.e. $P_{HR} = D_{HR}\alpha$. $\alpha$ can be optimized according to the following equation:

$$\min_{\alpha} = \|P_{LR} - \alpha D_{LR}\|_2^2 + \beta\|\alpha\|_1 \tag{4}$$

where $\beta$ is the parameter to balance fidelity and sparsity of the approximation of LR patch $P_{LR}$. The HR patch can be recovered as $P_{HR} = D_{HR}\alpha$. Equation (4) uses gradient decent to recover the required sparse representation $\alpha$. It has comparatively good results but its time complexity is very high and it cannot be incorporated in the applications that need real time response e.g. camera interpolation, theater etc.

Theory of edge detection plays a vital role in image SR techniques, so it is important to cover the concept of edges according to the human visual perception [11, 22, 36]. The mammalian visual cortex has evolved over millions of years to cope effectively with images of the natural environment. As the part of the cerebral cortex responsible for processing visual information, it is located in the occipital lobe. The term visual cortex refers to the primary visual cortex (also known as V1). V1 is the primary visual processing area in the cortex because LGN (Lateral Geniculate Nucleus) sends most of its axons to V1. Hubel and Wiesel discovered the functional organization and basic physiology of the neurons in V1 [13]. It consists of three different types of neurons called simple cells, complex cells and hyper-complex cells which transform information, i.e. orientation selective and direction selective [14]. Orientation selective means strong response to lines, bars or edges of particular orientation. Hubel & Wiesel's description of simple cells as linear with bar- or edge-shaped receptive fields led to a view of the cortex as containing a population of feature detectors tuned to edges and bars of various widths and orientations. Marr and Hildret [23] analyze a theory of edge detection in two parts. (1) Intensity changes are detected at different scales, which occur over a wide range of scales in a natural image. They proved that intensity changes at a given scale are best detected by computing the zero values of $\nabla^2 G(x, y)*S(x,y)$

for image *S*, where $\nabla^2$ is the Laplacian and *G(x, y)* is a two dimensional Gaussian. (2) Intensity changes in images arise from illumination boundaries or surface discontinuities from reflectance and these all have the property that they are localized spatially. It explains several basic psychophysical findings. The operation of forming oriented zero-crossing segments from the output of center-surround $\nabla^2 G$ filters acting on the image forms the basis for a physiological model of simple cell in the visual cortex. (see [23] for more details). In the proposed technique the properties of the human visual perception has been incorporated to produce better results qualitatively as quantitatively.

## 3 Proposed method

Suppose $S_{in}$ is the source image of size r×c and λ is a magnification factor. The source image is first expanded by factor λ. $S_{in}$ is mapped from a smaller pixel grid to larger pixel grid i.e. $S_{out}$ (R,C) = $S_{in}$(r×λ, c×λ) where R×C is the size of expanded image.

$$\widehat{S}_{out} = \begin{bmatrix} \lambda_x & 0 \\ 0 & \lambda_y \end{bmatrix} \begin{bmatrix} x_i \\ y_j \end{bmatrix} \tag{5}$$

where *x, y* are the coordinates and $\lambda_x$, $\lambda_y$ in Eq. (5) are the SR scales in horizontal and vertical directions, respectively. After expansion, $\widehat{S}_{out}$ has undefined pixels that are interpolated from already known pixels. In order to compute a suitable value for the undefined pixels, $\widehat{S}_{out}$ is convolved with a kernel $\Phi_{Gk}(s,t)$.

$$S_G(x,y) = \sum_{s=i} \sum_{t=j} \widehat{S}_{out}(x+s, y+t) \Phi_{Gk}(s,t) \tag{6}$$

$\Phi_{Gk}$(s,t) is the Gaussian kernel of size s×t. k denotes the type of Gaussian's kernel. In order to get the complete HR image to have appropriate values for undefined pixels, Eq. (6) must be convolved for x=1, 2 … R and y=1, 2 … C. The proposed technique uses two types of Gaussian kernels depending on the luminance information of the underlying interpolation window. The size of the interpolation window is also *s*×*t*. Initially, the standard deviation $\sigma_w$ of the interpolation window is computed as:

$$\sigma_w = \sqrt{\sum_{s=i} \sum_{t=j} \frac{\left(\mu - \widehat{S}_{out}(x+s, y+t)\right)^2}{s \times t}} \tag{7}$$

where $\mu$ is the mean of the interpolated window. The Gaussian Kernel is generated with $\sigma_{Gk}$=0.3 of size s×t, if $\sigma_w$ is greater than threshold τ otherwise it will be generated with $\sigma_{Gk}$=0.8 of the same size. The Gaussian kernel [10, 28, 37] is defined as:

$$\Phi_{Gk}(s,t) = \frac{1}{\sigma\sqrt{2\pi}} e^{\frac{-d^2}{2\sigma_{Gk}}} \tag{8}$$

where $d^2$ is the distance of neighboring pixels $(s_i, t_j)$ from the center pixel $(s_c, t_c)$. The $\sigma_{Gk}$ defines the width of a Gaussian kernel $\Phi_{Gk}(s,t)$ i.e. the degree of smoothness. In case of sharp luminance, we use the kernel with $\sigma_{Gk}$=0.3 and for smoothness where the interpolation region is constant, we use the kernel with $\sigma_{Gk}$=0.8. The values for $\sigma_{Gk}$={0.3, 0.8} have been chosen after a number of experiments on smoothed, textured and sharpened luminance interpolated regions of the images. $\sigma_{Gk}$ with value 0.3 gives good results on sharpened

luminance interpolated area while maintaining the texture of the image while $\sigma_{Gk}$ with value 0.8 has better quality for a smooth interpolated region. It preserves not only the smoothness of the image but also preserves the texture property of the image inside smooth regions. The Gaussian function has been shown with both sigma values in Fig. 1. The Gaussian kernels $\Phi_{Gk}(s,t)$ of size s×t generated with $\sigma_{Gk}$=0.3 and $\sigma_{Gk}$=0.8 are shown in Fig. 2. Figure 2a shows the interpolation window in the expanded image in the form of a grid of a size S×T. The dark gray blocks in the grid represent the known pixels and the white blocks in the grid stand for unknown pixels. The block containing '**X**' denotes the interpolated pixel. Both these kernels convolve to the known pixels inside the interpolation region and the sum of the convolved pixels is assigned to the block contain '**X**'.

The output image $S_G$ from Eq. (6) is further enhanced by deploying the properties of second order derivative. The second order derivative $\nabla^2$ has the substantial advantages of being isotropic, with a response that is independent of the orientation of sharp luminance variations (invariant to rotation) in the input image to which it is applied. These features of being isotopic not only according to human visual perception but also in reaction to changes in intensity equally in any mask direction. The simplest isotropic derivative operator 'Laplacian' can be defined for $S_G$ as

$$\nabla^2 S_G = \frac{\partial S_G}{\partial x} + \frac{\partial S_G}{\partial y} \tag{9}$$

The second order derivative is a linear operation [25]. In the $x$-direction, it can be expressed as

$$\frac{\partial S_G}{\partial x} = S_G(x+1,y) + S_G(x-1,y) - 2S_G(x,y) \tag{10}$$

and, similarly, in the y-direction it can be written as

$$\frac{\partial S_G}{\partial y} = S_G(x,y+1) + S_G(x,y-1) - 2S_G(x,y) \tag{11}$$

Thus the basic procedure in which Laplacian is used to enhance the quality of the output image is

$$S_{G+L} = S_G + k\left[\nabla^2 S_G\right] \tag{12}$$

where constant k=−1 and $\nabla^2 S_G$ highlights the discontinuities of luminance in $S_G$ and deemphasizes regions with slowly changes luminance levels. It also recovered the missing background features while preserving the sharpness of the output

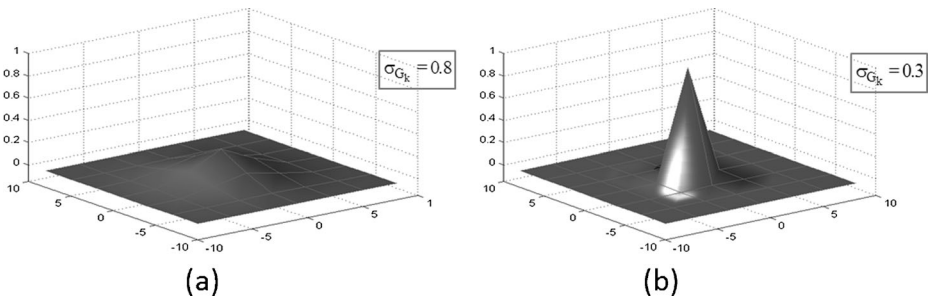


**Fig. 1** The two-dimensional Gaussian function with $\sigma_{Gk}$=0.8 *and* $\sigma_{Gk}$=0.3

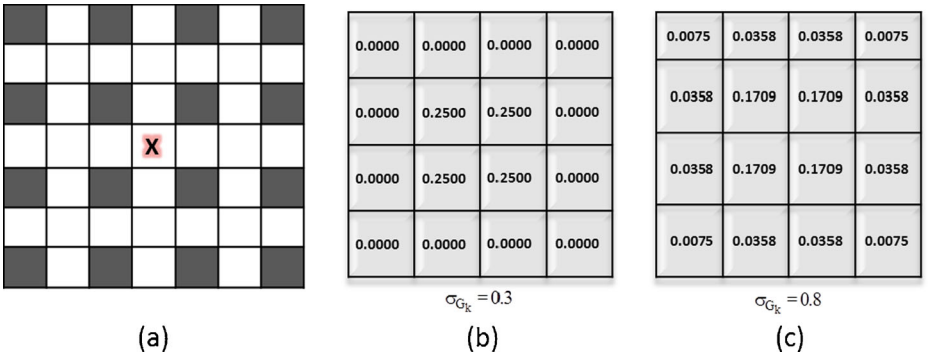


**Fig. 2** (**a**) Example of interpolation window in expanded image (**b**) is the Gaussian kernel with $\sigma_{Gk}$=0.3 (**c**) is the Gaussian kernel with $\sigma_{Gk}$=0.8

image $S_{G+L}$. In order to bring the magnified image closer to the original image, $S_{G+L}$ and $S_G$ are averaged as

$$S_{out} = \frac{(S_G + S_{G+L})}{2} \tag{13}$$

The intensity of $S_{G+L}$ can be specified in the range [0-$f_m$] (e.g. for unsigned 8-bit integer $f_m$=255 and for double-precision floating point $f_m$=1). Extensive experimental results validate the superiority of the proposed technique over state-of-the-art techniques. Figure 3 shows the system model of the proposed technique. The proposed technique takes a gray-scale image as an input and produces the zoomed image by factor λ. It also works the same for a color image. Let $£_{rgb}$ be the color source input image of size r×c×z where z stands for RGB color channels. We split this color image $£_{rgb}$ into RGB channels e.g. $£_r$, $£_g$ and $£_b$. On each separate color channel (gray-scaled image) the proposed technique is applied independently with magnification λ and produced the magnified images of each color channel $£_R$, $£_G$ and $£_B$ of size R×C. For combining these three $£_R$, $£_G$ and $£_B$ images we get the zoomed color image $£_{RGB}$ of size R×C×Z.

## 4 Experimental results

The proposed technique has been evaluated qualitatively as well as quantitatively using various image quality assessment metrics. For this purpose we use a set of images downloaded from a public database [1–3]. The images taken from 'McGill Calibrated Color Image Database' (MGD) [2] are in TIF format with sizes of 786×576. The images were downloaded from the websites of Computer Vision Group (CVG), University of Granada [1] and Center for Image Processing Research (CIPR) of Rensselaer Polytechnic Institute [25], and are in PBM or PGM format with sizes of 768×512 and Kodak format of sizes 512×512 respectively. The size and format of the underlying image can be adjusted according to the requirement of the experiment. All the images used for quantitative analysis were adjusted to single format PGM and to size R×C where R = C=512. First, the images were reduced by factor λ=1/4 and then magnified to original size using different zooming techniques. Let $S_{in}$ be the original image obtained from public database and $S_{out}$ is the magnified output image after

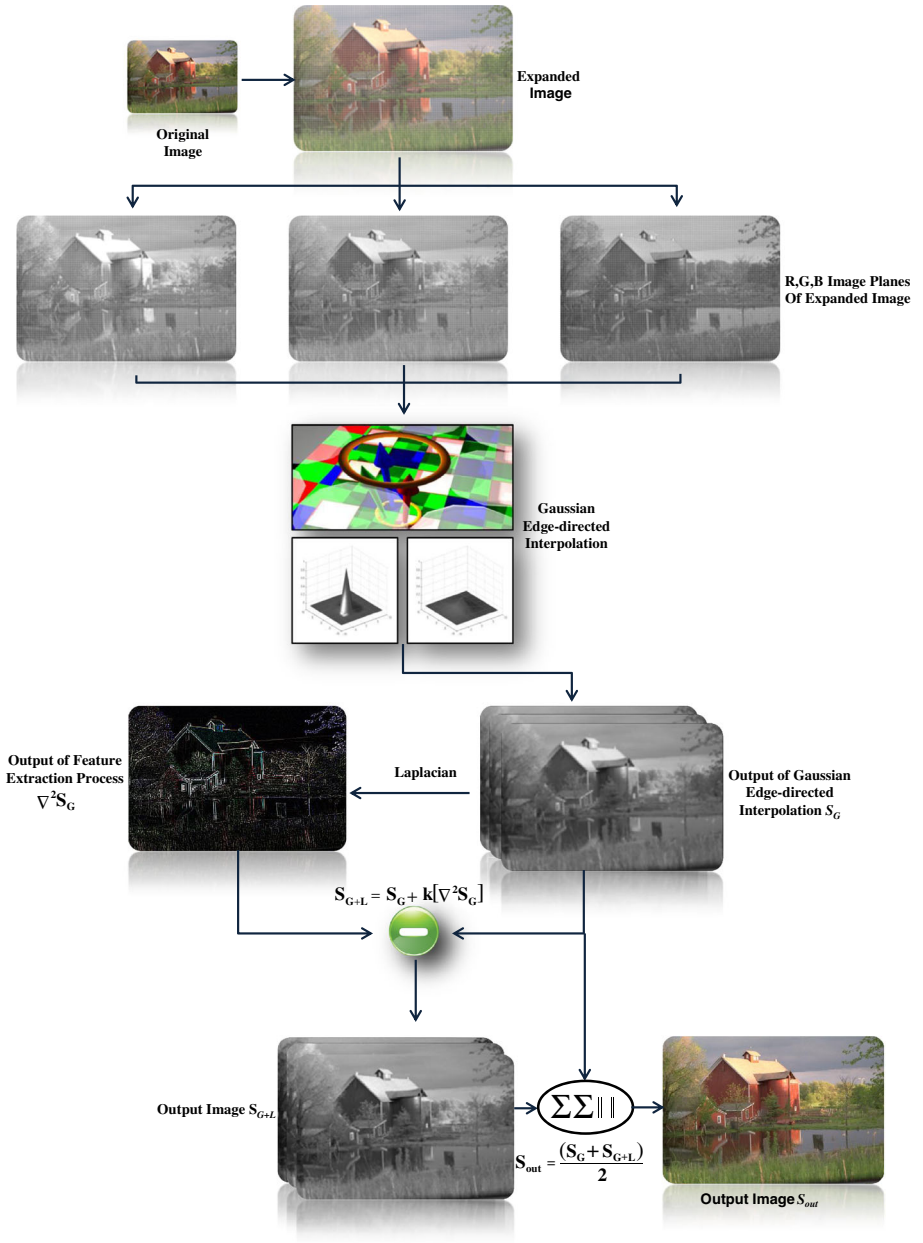


**Fig. 3** System model of the proposed image SR scheme

reducing it by λ=1/4. The proposed technique has been compared quantitatively and as well as qualitatively with four other techniques; one recent technique 'IIn' [18] and the other three are well-known classic interpolation schemes i.e. Nearest Neighbor (NN), Bilinear and Bicubic interpolation techniques [5]. The software package for IIn was provided by the author and for NN, bilinear and bicubic we used existing implementations in MATLAB R2011b.

### 4.1 Quantitative evaluation methods

In order to evaluate that how much the magnified image $S_{out}$ resembles the original image $S_{in}$ in quality, three evaluation methods; peak signal to noise ratio (PSNR) [18], cross correlation coefficient (CC) [7] and structural similarity index method (SSIM) [34] have been used to assess the quality of the output image. The software package of SSIM can be downloaded from the Image/Video quality database [29]. PSNR evaluates the quality of the output image by computing the strength of the corrupting noise and the maximum achievable power of the signal. The noise introduced during the zooming process weakens the signal by reducing the maximum achievable power of the original signal. It approximates the superiority of the zooming technique with respect to human visual perception. The higher value of the PSNR indicates higher quality and vice versa. PSNR can be calculated as

$$PSNR = 20*\log_{10}\frac{\mathrm{I}_{max}}{MSE} \tag{14}$$

$$MSE = \frac{\sum_{i=1,j=1}\left(S_{in}\left(x_i,y_j\right)-S_{out}\left(x_i,y_j\right)\right)^2}{RC} \tag{15}$$

where $I_{max}$ in Eq. (14) is the maximum intensity fluctuation in the input image data type (e.g. for unsigned 8-bit integer $I_{max}$=255 and for double-precision floating point $I_{max}$=1). CC computes the cross correlation between the input image $S_{in}$ and the output image $S_{out}$. It indicates how much the calculated signal is related to the original signal. It computes values in the range [0–1]. The values nearest to 1, are highly related and vice versa. CC can be computed as

$$CC = \left[\frac{\left(\sum_{i=1,j=1} S_{in}\left(x_i,y_j\right)S_{out}\left(x_i,y_j\right)-RC\mu_{S_{in}}\mu_{S_{out}}\right)}{\left(\sum_{i=1,y=1} S_{in}^2\left(x_i,y_j\right)-RC\mu_{S_{in}}^2\right)\left(\sum_{i=1,j=1} S_{out}^2\left(x_i,y_j\right)-RC\mu_{S_{out}}^2\right)}\right] \tag{16}$$

Sometimes, *PSNR* does not compute the right value to assess the quality of the magnified image and it deviates from the ground truth. Therefore, *SSIM* is incorporated to evaluate the quality of the zoomed image. It adjusts according to human visual perception while assessing the quality of the magnified image. It computes the local statistical features of the magnified signal. It is very sensitive to noise because it focuses on the distortion of the structural contents of the input image. *SSIM* of the magnified image is computed as

$$SSIM = \frac{\left(2\mu_{S_{in}}\mu_{S_{out}}+C_1\right)\left(2\sigma_{S_{in},S_{out}}+C_2\right)}{\left(\mu_{S_{in}}^2+\mu_{S_{out}}^2+C_1\right)\left(\sigma_{S_{in}}^2+\sigma_{S_{out}}^2+C_2\right)} \tag{17}$$

where σ is the variance or the covariance of the $S_{in}$ and $S_{out}$ and $C_1$, $C_1$ are two variables for stabilizing the division with a weak denominator. The local statistics of the *SSIM* are computed within a kernel of size 8×8. It computes values in the range [−1 1]. The value closed to 1 shows high quality and vice versa. The matlab implementation of SSIM can be downloaded from [29].

### 4.2 Analysis of quantitative results

In this sub-section, we analyze the results obtained by evaluation metrics discussed in the previous section. The results computed by PSNR have been shown in Table 1. The proposed technique has the highest PSNR values, which show the superiority of the proposed technique over other techniques. The proposed technique improves the power of the achievable signal while magnifying the signal of the input image. NN has the lowest scores for PSNR. The PSNR results of Bilinear and IIn are close to each other. The proposed technique surpasses the bicubic most of the time.

Table 2 shows scores of CC for the proposed scheme, NN, bilinear, bicubic and IIn. The scores of the proposed technique are very close to classic bicubic in that they are almost equal. The scores of bilinear is slightly higher than IIn. NN and IIn have approximately the same cross correlation results. The statistics in Table 2 indicate that the signal magnified by the proposed technique has a high correlation with the original signal as that of the bicubic interpolation scheme.

In Fig. 4, the results of the proposed scheme show a higher structural similarity than other zooming schemes. NN has the lowest score for SSIM. The scores of classic bicubic interpolation schemes are higher than IIn and bilinear but less than that of the proposed technique. The proposed scheme computes the local statistical features of the magnified signal close to the original signal. It also frees the structural contents of the magnified image from distortions. The overall results of the proposed technique are better than other zooming techniques and it shows that the proposed technique calculates the unknown value close to the original value. This is because of two separate Gaussian kernels used adaptively and the proper usage of Laplacian.

### 4.3 Visual analysis

In this sub-section, we evaluate the visual quality of the proposed scheme by comparing it with other magnification schemes e.g. bilinear, bicubic, IIn. NN has been excluded from visual analysis because of its low visual quality. To examine the visual results of the proposed technique alone, different images were zoomed with different magnification factors. In Fig. 5, a cropped portion of size 146× 54 (Fig. 5a) from the color image of a bobcat has been magnified by factor $\lambda=2$ (Fig. 5b) and by factor $\lambda=4$ (Fig. 5c). The proposed technique preserved the texture, edges, smoothness, and geometrical variation of the zoomed image to the greaterest extent, which

**Table 1** Comparison of the proposed technique with other zooming techniques by calculating PSNR using Eq. (14) over 10 standard images. Zooming factor $\lambda=4$

| No. | Image name | NN | BL | BC | IIn | Proposed |
|---|---|---|---|---|---|---|
| 1 | Harbor | 20.65 | 25.11 | 26.44 | 24.45 | 27.35 |
| 2 | Cameraman | 26.48 | 21.22 | 22.42 | 20.34 | 22.67 |
| 3 | House | 20.58 | 27.83 | 28.38 | 26.43 | 29.36 |
| 4 | Avion | 21.57 | 31.78 | 33.23 | 31.20 | 34.43 |
| 5 | Baboon | 19.78 | 21.45 | 22.27 | 20.54 | 23.42 |
| 6 | Athens | 20.11 | 26.54 | 28.52 | 26.92 | 29.67 |
| 7 | Barbara | 18.89 | 22.63 | 23.24 | 21.57 | 25.81 |
| 8 | Boat | 21.71 | 25.36 | 26.29 | 22.36 | 27.47 |
| 9 | Peppers | 25.14 | 27.54 | 28.85 | 27.13 | 31.43 |
| 10 | Lena | 23.25 | 27.21 | 29.43 | 27.43 | 31.32 |
| | Average | 21.81 | 25.66 | 26.90 | 24.80 | 28.28 |

**Table 2** Comparison evaluation of the proposed technique with NN, bilinear, bicubic, and IIn by computing CC using equation (16)

| No. | Image name | NN | Bilinear | Bicubice | IIn | Proposed |
|---|---|---|---|---|---|---|
| 1 | Harbor | 0.86 | 0.88 | 0.91 | 0.86 | 0.92 |
| 2 | Cameraman | 0.87 | 0.92 | 0.95 | 0.88 | 0.95 |
| 3 | House | 0.84 | 0.90 | 0.93 | 0.84 | 0.94 |
| 4 | Avion | 0.84 | 0.89 | 0.90 | 0.84 | 0.91 |
| 5 | Baboon | 0.85 | 0.87 | 0.92 | 0.86 | 0.92 |
| 6 | Athens | 0.85 | 089 | 0.91 | 0.85 | 0.92 |
| 7 | Barbara | 0.91 | 0.93 | 0.97 | 0.94 | 0.96 |
| 8 | Boat | 0.91 | 0.93 | 0.94 | 0.92 | 0.95 |
| 9 | Peppers | 0.89 | 0.91 | 0.96 | 0.92 | 0.96 |
| 10 | Lena | 0.90 | 0.92 | 0.95 | 0.93 | 0.96 |
| | Average | 0.87 | 0.90 | 0.93 | 0.88 | 0.93 |

proved its high quality. In Fig. 6, the cropped portion with a size of 61×55 of a fingerprint gray-scale image (Fig. 6a) has been magnified by factor λ=2 (Fig. 6b) and by factor λ=4(Fig. 6a). The magnified images show the high quality of the proposed zooming scheme. Now, the visual results of the proposed scheme are evaluated against other mentioned zooming techniques as shown in Figs. 7 and 8. These visual results show that the proposed technique preserves the sharp luminance information across the boundaries. It also preserves the texture of the magnified image. Moreover, it reduces unwanted artifacts to a greater extent, which is the main property of a good magnification technique. Other techniques produce numerous problems in zoomed versions of the input image, such as blurring and blocking effects across the edges. These schemes also fail to preserve both geometrical regularities as well as textures inside the regions of high frequencies, which consist of original details of the reference image. They also create ghosting effects in the regions of high contrast which can be observed in the visual results of IIn. Visual analysis is concluded by claiming that the quality of the proposed technique is comparatively better than the other three mentioned zooming schemes i.e. bilinear, bicubic and IIn. The running time of the proposed scheme is also assessed with respect to other schemes. The time complexity of the proposed technique is simple as that of bicubic interpolation i.e. O(R, C) where R is the number of rows and C is the number of columns. The average execution time of all mentioned zooming

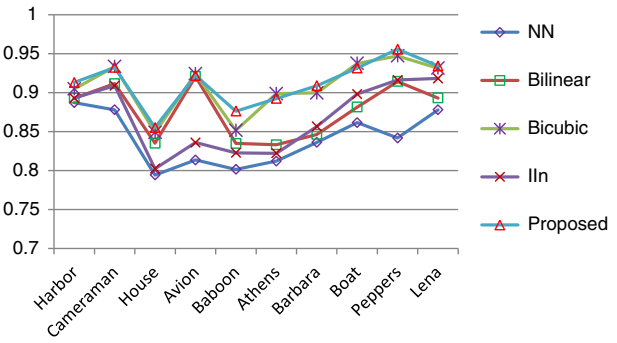


**Fig. 4** SSIM computed over ten images zoomed by factor λ=4 using proposed technique, bilnear, bicubic and IIn zooming techniques

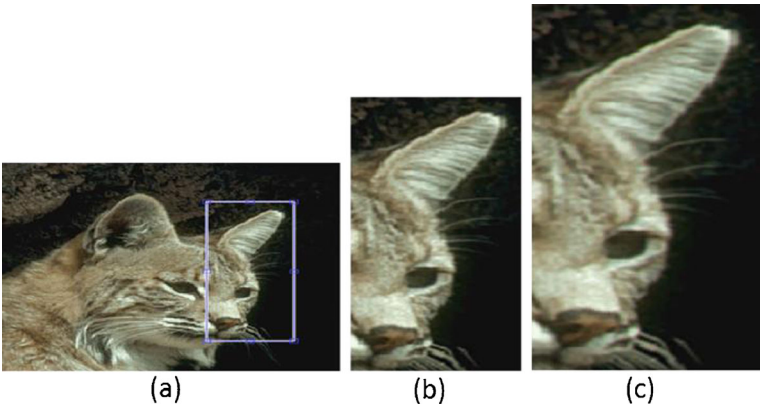


**Fig. 5** (**a**) Cropped portion of size 194×71 of a bobcat. (**b**) 2× and (**c**) 4× zoomed by the proposed scheme

techniques over ten standard images are given in Fig. 9. The images were zoomed with factor λ=4. The execution time comparison was conducted using an Intel Core 2 Duo processor T7800 (2.6GHz), 4GB DDR2 shared 667 MHz over MATLAB R2011b version. The graph shows that the execution time of the proposed technique is close to Bicubic technique. Bicubic is an non-adaptive technique and the proposed technique is adaptive.

Both qualitative and quantitative results show the superiority of the proposed technique over NN, bilinear bicubic and IIn. The proposed technique produces less error while magnifying the signal. The interpolator of the proposed scheme maintains both geometrical regularities as well as texture inside the regions of high frequencies, which consist of original details of the source input image. Particularly, conventional interpolation schemes e.g. bilinear and bicubic are non-adaptive and use only one interpolation kernel, which produce noise and blurring effects during the interpolation process. The proposed scheme is adaptive because it switches between different Gaussian edge-directed kernels by considering the underlying sharp luminance information. It also enhances the quality of the output image by applying Eqs. (12) and (13). Hence the proposed technique produces high quality at a low cost.


**Fig. 6** (**a**) 61×55 cropped portion enclosed by rectangle (**b**) magnified using the proposed scheme by factor λ=2 and (**b**) λ=4

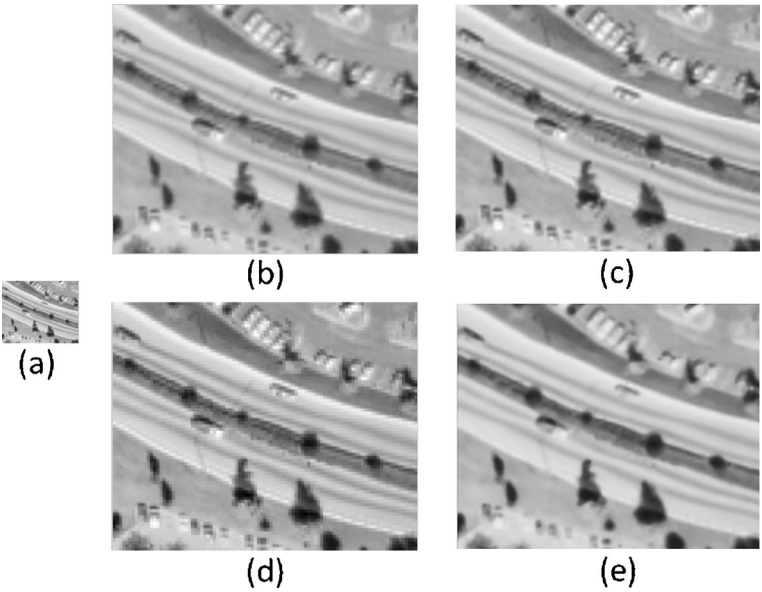


**Fig. 7** (**a**) Cropped portion of size 88×69 from areal image. Zoomed 4 times using (**b**) bilinear, (**c**) bicubic, (**d**) IIn, and (**e**) the proposed technique

## 5 Conclusion

In this paper we have presented a digital image SR scheme via a Gaussian edge-directed interpolation method. The proposed technique uses different Gaussian kernels that intelligently calculate the weights of the neighboring pixels in the premises of the interpolated pixel. The standard deviation of the interpolation window decides the type of Gaussian kernel to be used according to the underlying intensity information. The Gaussian kernel with $\sigma_{Gk}$=0.3 works well in high frequencies and maintains the sharp luminance variations across the boundaries in the generated image. The Gaussian kernel with $\sigma_{Gk}$=0.8 works well in the regions containing similar and consistent luminance intensity information. It maintains the smoothness and texture information inside the boundaries of high frequencies in the output image. The second order derivative $\nabla^2$ is applied to the image obtained by applying the Gaussian kernel. It has various advantages by

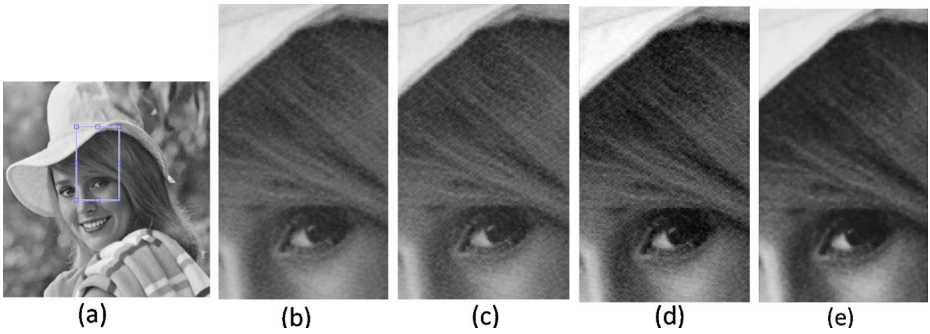


**Fig. 8** (**a**) Cropped portion of size 100×52 from standard Elaine image. Magnified by factor λ=4 using (**b**) bilinear, (**c**) bicubic, (**d**) IIn, and (**e**) the proposed zooming techniques

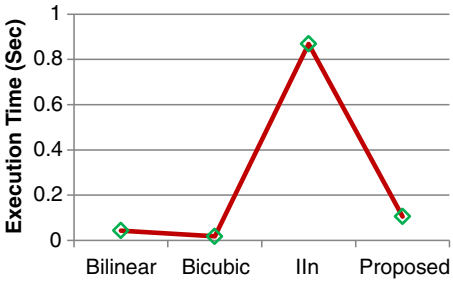


**Fig. 9** Average execution time (in seconds) over ten standards images zoomed by factor λ=4

having the property of being isotropic i.e. it is invariant to rotation in all directions. This property of being isotropic of the second order derivative $\nabla^2$ is not only according to human visual perception but also has the capability to react in all directions equally irrespective of the underlying filter. It has the response properties resembling the simple cells of the visual cortex. The processing procedure of the Laplacian $\nabla^2$ is close to human visual perception. Due these properties, $\nabla^2$ highlights the geometrical variations and deemphasizes the areas carrying low-intensities in an HR image generated by the adaptive kernel of the proposed technique. It also highlights the missing features in the background while preserving the contrast of the output image. Hence, the HR image produced by the proposed scheme is of high quality because it maintains the geometrical regularities of the original input image. It also preserves the smoothness and texture inside the high frequencies across the boundaries. Extensive experimental comparisons with state-of-the-art magnification techniques confirm the effectiveness of the proposed technique.

In the experimental section, both qualitative and quantitative comparisons with state-of-the-art methods have been conducted. Various quantitative evaluation metrics have been used to assess the quality of the proposed schemes. The statistics of CC proved that the proposed technique computes the interpolated pixel to be very close the original pixel compared to other zooming schemes. Therefore, the signal magnified by the proposed scheme has the maximum achievable power in contrast to other mentioned schemes assessed by the evaluation metric PSNR. SSIM validates that the proposed scheme has a higher structural similarity with more original detail of the reference image than NN, bilinear, bicubic and IIn. The visual comparisons also endorse the superiority of the proposed technique.

In spite of this, the proposed scheme has certain limitations. It is good at preserving edges but fails to distinguish the signal from noise, and so the results contain some unwanted artifacts i.e. it cannot conduct denoising and magnification simultaneously. The second order derivative $\nabla^2$ covers the response properties of simple cells of the primary visual cortex at a minute level. Features extracted by the second order derivative resemble the response properties of receptive fields of a few neurons in the primary visual cortex. The visual cortex contains a large amount of feature descriptors. Moreover, two Gaussian kernels are not sufficient to recover the full original details of the input image.

In the future, we intend to incorporate the above limitations as modifications to the proposed scheme. In order to enable the proposed technique to handle image SR and denoising simultaneously, the set of feature descriptors can be replicated from the response behaviors of the receptive fields of neurons in the visual cortex at various levels. These feature descriptors can be combined in the form of a dictionary. Compress sensing and sparse coding can be very useful in this regard. As machine learning algorithms have a high time complexity, it can be reduced by using some numerical shortcuts e.g. dimensionality reduction via principal component analysis.

Moreover, we intend to test the interpolation region for more than two Gaussian kernels with different values of $\sigma_{Gk}$ to preserve the details of the original image to a greater extent.

**Acknowledgments** This research is supported by: (1) Basic Science Research Program through the National Research Foundation of Korea (NRF) funded by the Ministry of Education (2013R1A1A2012904). (2) Industrial Strategic technology development program, 10041772, (The Development of an Adaptive Mixed-Reality Space based on Interactive Architecture) funded by the Ministry of Trade, Industry and Energy' (MOTIE).

## References

1. [Online]. Available: http://decsai.ugr.es/cvg/dbimagenes/g512.php
2. [Online]. Available: http://pirsquared.org/research/mcgilldb/
3. [Online]. Available: http://www.cipr.rpi.edu/resource/stills/kodak.html
4. Acharya T, Tsai P (2007) Computational foundations of image interpolation algorithms, ACM Ubiquity 8:1–17
5. Amanatiadis A, Andreadis I (2009) A survey on evaluation methods for image interpolation. Meas Sci Technol 20(10):104015–104021
6. Baker S, Kanade T (2002) Limits on super-resolution and how to break them. IEEE Trans Pattern Anal Mach Intell 24:1167–1183
7. Battiato S, Gallo G, Stance F (2002) A locally adaptive zooming algorithm for digital images. Image Vision Comput 20:805–812
8. Ejaz N, Tariq TB, Baik SW (2012) Adaptive key frame extraction for video summarization using an aggregation mechanism. J Visual Commun Image Represent 23(7):1031–1040
9. Gajjar PP, Joshi MV (2010) New learning based super-resolution: use of DWT and IGMRF prior. IEEE Trans Image Process 19(5):1201–1213
10. Gonzalez RC, Woods RE (2007) Digital image processing 3rd edn, Amazon
11. He H, Siu W-C (2011) Single image super resolution using Gaussian process regression, 2011 IEEE Conf Comput Vision Pattern Recognit pp 449–456
12. Hou HS, Andrews HC (1978) Cubic splines for image interpolation and digital filtering. IEEE Trans Acoustics, Speech Signal Proc 26:508–517
13. Hubel DH (1959) Single unit activity in striate cortex of unrestrained cats. J Physiol 147:226–238
14. Hubel DH, Wiesel TN (1969) Visual area of the lateral suprasylvian gyrus (Clare—Bishop area) of the cat. J Physiol 202:251–260
15. Hung KW, Siu WC (2009) New motion compensation model via frequency classification for fast video super-resolution, IEEE Int Conf Image Process
16. Hwang JW, Lee HS (2004) Adaptive image interpolation based on local gradient features. IEEE Signal Process Lett 11:359–362
17. Irani M, Peleg S (1993) Motion analysis for image enhancement: resolution, occlusion and transparency. J Visual Commun Image Represent 4(4):324–335
18. Jurio A, Pagola M, Mesiar R, Beliakov G, Bustince H (2011) Image magnification using interval information. IEEE Trans Image Process 20(11):3112–3123
19. Kim KI, Kwon Y (2008) Example-based learning for single image super-resolution and jpeg artifact removal. Technical report 173, Max Planck Institute
20. Lee YJ, Yoon J (2010) Nonlinear image upsampling method based on radial basis function interpolation. IEEE Trans Image Process 19(10):2682–2692
21. Li X, Orchard MT (2001) New edge-directed interpolation. IEEE Trans Image Process 10:1521–1527
22. Mallat S, Yu G (2010) Super-resolution with sparse mixing estimators. IEEE Trans Image Process 19(11):2889–2900
23. Marr D, Hildreth E (1980) Theory of edge detection. Proc R Soc London, Ser B 207:187–217
24. Ni KS, Nguyen TQ (2007) Image super resolution using support vector regression. IEEE Trans Image Process 16(6):1596–1610
25. Rosenfeld A, Kak AC, Rosenfeld A, Kak AC (1982) Digital picture processing, vol 1, 2nd edn. Academic, New York
26. Sajjad M, Ejaz N, Baik SW (2012) Multi-kernel based adaptive interpolation for image super-resolution. Multimed Tools Appl. doi:10.1007/s11042-012-1325-4
27. Shan Q, Li Z, Jia J, Tang CK (2008) Fast image/video upsampling. ACM Trans Graphics (SIGGRAPH ASIA) 27:153–160
28. Shapiro LG, Stockman GC (2001) Computer vision, Amazon

29. Sheikh HR, Wang Z, Bovik AC, Cormack LK. Image and video quality assessment research at LIVE http://live.ece.utexas.edu/research/quality/
30. Srinivasan U, Pfeiffer S et al (2005) A survey of MPEG-1 audio, video and semantic analysis techniques. Multimed Tools Appl 27:105–141
31. Suzuki J, Furukawa I (2000) Application of super high definition images in telemedicine: system requirements and technologies for teleradiology and telepathology. Multimed Tools Appl 12:7–38
32. Tam WS, Kok CW, Siu WC (2010) A modified edge directed interpolation for images. J Electronic Imaging 19(1):1–20
33. Tian Y, Yap KH, He Y (2012) Vehicle license plate super-resolution using soft learning prior. Multimed Tools Appl 60:519–535
34. Wang Z, Bovik AC, Sheikh HR, Simoncelli EP (2004) Image quality assessment: from error visibility to structural similarity. IEEE Trans Image Process 13(4):600–612
35. Wittman T (2005) Mathematical techniques for image interpolation, Department of Mathematics University of Minnesota
36. Yang J, Wright J, Huang TS, Ma Y (2010) Image super-resolution via sparse representation. IEEE Trans Image Process 19(11):2861–2873
37. Yeon JL, Jungho Y (2010) Nonlinear image upsampling method based on radial basis function interpolation. IEEE Trans Image Process 19(10):2682–2692

**Muhammad Sajjad** received his MS degree in Computer Software Engineering from National University of Sciences and Technology, Pakistan. He is currently pursuing PhD course in Sejong University, Seoul, Korea. His research interests include digital image magnification and reconstruction, Sparse coding, video quality assessment and video retrieval.

**Naveed Ejaz** received his MS degree in Computer Software Engineering from National University of Sciences and Technology, Pakistan. He is currently pursuing PhD course in Sejong University, Seoul, Korea. His research interests include digital image and video retrieval, video summarization, and video analytics.

**Irfan Mehmood** received his BS degree in Computer Science from National University of Computer and Emerging Sciences from Pakistan. He is currently pursuing his Ph.D. degree at Sejong University, Seoul, Korea. His research interests include video summarization, medical image processing, and computer vision.

**Sung Wook Baik** is a professor in the Department of Digital Contents at Sejong University. His research interests include Computer vision, Pattern recognition, Computer game and AI. He has a PhD in Information Technology and Engineering from George Mason University.